HHS Public Access

Author manuscript

Br J Ophthalmol. Author manuscript; available in PMC 2017 March 01.

Published in final edited form as:

Br J Ophthalmol. 2016 March ; 100(3): 295–299. doi:10.1136/bjophthalmol-2015-307105.

Volumetric Ellipsoid Zone Mapping for Enhanced Visualization of Outer Retinal Integrity with Optical Coherence Tomography

Yuji Itoh, MD, PhD[1], **Amit Vasanji, PhD**[2], and **Justis P. Ehlers, MD**[1]

[1]Ophthalmic Imaging Center; Cole Eye Institute, Cleveland Clinic, Cleveland, Ohio, USA

[2]ImageIQ, Cleveland, Ohio USA

Abstract

Objective assessment of retinal layer integrity with optical coherence tomography (OCT) is currently limited. The ellipsoid zone (EZ) has been identified as an important feature on OCT that has critical prognostic value in macular disorders. In this report, we describe a novel assessment tool for EZ integrity that provides visual and quantitative assessment across an OCT data set. Utilizing this algorithm, we describe the findings in multiple clinical examples, including normal controls, age-related macular degeneration, drug effects (e.g., ocriplasmin, hydroxychloroquine), and effects of surgical manipulation (e.g., following membrane peeling utilizing intraoperative OCT). EZ mapping provides both *en face* visualization of EZ integrity and EZ-retinal pigment epithelium height. Additionally, volumetric, area, and linear measurements are feasible using this assessment tool.

Introduction

In the past decade, optical coherence tomography (OCT) has transformed the diagnostic approach to numerous vitreoretinal diseases. Spectral domain OCT (SDOCT) has allowed for outstanding visualization of numerous retinal structures. The outer retina is characterized by four highly reflective bands that can be seen on SDOCT in the normal eye [i.e., external limiting membrane (ELM), ellipsoid zone (EZ), interdigitation zone (IZ, or cone outer segment tips) and retinal pigment epithelium (RPE)].[1–3] The EZ and ELM, in particular, have been linked to visual outcomes and prognosis in numerous macular conditions, such as age-related macular degeneration (AMD), hydroxychloroquine toxicity, and intravitreal ocriplasmin injection.[4–10] Objective evaluation of the EZ has been lacking. The purpose of this report was to evaluate a novel analysis tool for EZ mapping with *en face* visualization and volumetric assessment in numerous retinal conditions as a potential platform for potential future research and clinical applications.

Correspondence: Justis P. Ehlers, Cole Eye Institute, Cleveland Clinic, 9500 Euclid Avenue, i30, Cleveland, Ohio 44195, USA; ehlersj@ccf.org.

Disclosures:

NIH/NEI K23-EY022947-01A1 (**JPE**); Ohio Department of Development TECH-13-059 (**JPE**); Research to Prevent Blindness (**Cole Eye Institutional Grant**); Machemer Foundation Fellowship (**YI**)

YI: None;

AV: None;

JPE: Bioptigen (C,P), Thrombogenics (C, R), Synergetics (P), Genentech (R), Leica (C), Carl Zeiss Meditec (C), Alcon (C)

Methods

Cleveland Clinic IRB-approval was obtained for a retrospective assessment of eyes undergoing SDOCT testing with a novel EZ mapping tool. Initial conditions selected for evaluation included normal controls, geographic atrophy secondary to age-related macular degeneration, hydroxychloroquine toxicity, ocriplasmin-related EZ attenuation, and outer retinal dynamics following membrane peeling. These conditions were selected due to the predominance of outer retinal alterations. Additionally, for initial assessment purposes, conditions with minimal RPE disturbance were selected.

An automated EZ mapping tool was developed at the Ophthalmic Imaging Center at Cleveland Clinic through collaboration with ImageIQ (Cleveland, OH) for segmenting the EZ with additional retinal layers, providing linear, area, and volumetric measurements, as well as *en face* visualization for evaluating EZ and outer retinal dynamics (Figure 1). In brief, the macular cube data set was imported into a novel OCT automated segmentation tool. Automated segmentation and mapping was performed. The SDOCT image stack was passed through multiple filters and the RPE was identified as the floor for the algorithm segmentation. Utilizing a prespecified search area, the EZ was identified, if present, based on relative intensity, proximity and relative location of the outer retinal bands. Manual independent reviewer of the segmentation accuracy was performed for each of the eyes. To evaluate reliability of the algorithm, multiple time points in normal samples were assessed and compared for variability. The data set was the then transformed into multiple output components. Cross-sectional area and cubic volumetric data was generated related to the EZ-RPE thickness. Three-dimensional reconstruction was also performed of the entire dataset with embedded EZ-mapping for visualization of areas of pathology. Finally, *en face* EZ thickness topographic maps were created for each dataset. Zeiss Cirrus SD-OCT system was utilized for all normal, AMD, hydroxychlorquine, and ocriplasmin eyes with a 6 mm × 6 mm macular cube. The intraoperative OCT scan assessment following membrane peeling was performed with the Bioptigen Envisu system with a 10 mm × 10 mm macular cube.

Results

A total of 34 eyes were included in this innovation report. Twelve normal eyes were assessed with the EZ mapping algorithm. The mean EZ-RPE volume was 1.27 ± 0.094 (mm^3), the mean central foveal area was 0.22 ± 0.019 (mm^2) and mean EZ map thickness was > 20 microns in 99% of sampled areas. Multiple time points were assessed in 11 normal eyes to evaluate the algorithm reproducibility. The mean EZ volume at the first and second visit were highly correlated [1.26 ± 0.094 (mm^3) and 1.28 ± 0.11 (mm^3), correlation coefficient = 0.82, $P < 0.001$).

EZ mapping in AMD with geographic atrophy (n = 4) exhibited multi-focal areas of EZ loss on the *en face* map and decreased EZ-RPE volume (Figure 2). EZ-RPE volume was reduced to a mean of 1.02 ± 0.17 mm^3 (P = 0.015, compared to normal cases) and an EZ thickness of > 20 microns was seen in only (59–89%) of the cube compared to 99% in normal eyes reflecting the areas of atrophy.

Mild hydroxychloroquine toxicity (n = 3) EZ mapping exhibited the expected concentric thinning of the EZ-RPE thickness with associated foveal sparing. In a representative case (Figure 3), EZ-RPE volume and area were reduced compared to normals (0.93 mm^3 and 0.17 mm^2 respectively). The EZ map showed significant reduction EZ integrity with a mean EZ thickness of > 20 microns in only 80% of sampled areas.

Ocriplasmin-related outer retinal attenuation (n =15) showed variable EZ attenuation and thinning (Figure 4). In a representative case, EZ mapping revealed reduction of EZ-RPE volume to 0.15 mm^3. EZ thickness of > 20 microns was present in only 52% of sampled areas on EZ *en face* maps.

EZ-mapping was also performed on intraoperative OCT scans before and after internal limiting membrane peeling. Prior to ILM peeling the EZ-RPE volume was 2.94 mm^3 and after ILM was increased dramatically to 4.7 mm^3. This was reflected in the *en face* EZ map (Figure 5).

Discussion

This study represents a new innovation in OCT assessment of relative retinal layer analysis with particular focus on the EZ and outer retina. In-depth visualization utilizing EZ mapping allows for overall volumetric assessment and topographic visualization of the relative locations of EZ alterations. In this report, we utilize the novel tool for evaluation of numerous macular conditions.

In normal eyes, the EZ maps revealed excellent EZ integrity with high repeatability. In eyes after intravitreal ocriplasmin, geographic atrophy, and hydroxychloroquine toxicity EZ mapping successfully identified EZ-RPE alterations. Not only could this be assessed on a volumetric scale, but topographic representations of the *en face* EZ map allowed for pattern based analysis and identification. This may be particularly useful in subtle bulls-eye patterns (such as subclinical hydroxychloroquine toxicity) and for multifocal extrafoveal atrophy, such as in early geographic atrophy. Change analysis of thickness maps may also be particularly useful in understanding retinal dynamics and alterations that occur during various disease processes or following therapeutic interventions. For example, alterations in the EZ-RPE relationship following ILM peeling identified on intraoperative OCT predicted speed of anatomic normalization in macular hole repair.[11] Utilizing the EZ mapping system, rapid quantitative assessment of intraoperative alterations may be feasible that prognosticates macular hole normalization rate.

This report has some important limitations, including its small sample size and its retrospective nature. Further prospective research with larger numbers including normal eye, various retinal diseases are needed to assemble a normative database. However, the utility of an objective quantitative assessment tool for EZ integrity for clinical trials and disease prognostication/management may prove particularly useful. This report was primarily limited to conditions that more focally impact the outer retina with a minimally disturbed RPE. Expansion of the assessment tool is needed into more complex pathologies, such as

choroidal neovascularization and conditions associated with macular edema (e.g., diabetic macular edema). This research is ongoing.

This report describes a novel technology and visualization tool for the quantitative assessment of the EZ and EZ-RPE thickness utilizing both volumetric and *en face* tomographic representations. Additional research is needed to further assess the utility of the tool in various pathologic conditions, as well as more in-depth integrative pattern analysis is needed to better assess this tool as a disease modeling and diagnosis guidance tool.

References

1. Srinivasan VJ, Monson BK, Wojtkowski M, et al. Characterization of outer retinal morphology with high-speed, ultrahigh-resolution optical coherence tomography. Invest Ophthalmol Vis Sci. 2008 Apr; 49(4):1571–9. [PubMed: 18385077]
2. Staurenghi G, Sadda S, Chakravarthy U, et al. Proposed lexicon for anatomic landmarks in normal posterior segment spectral-domain optical coherence tomography: the IN•OCT consensus. Ophthalmology. 2014 Aug; 121(8):1572–8. [PubMed: 24755005]
3. Spaide RF, Curcio CA. Anatomical correlates to the bands seen in the outer retina by optical coherence tomography: literature review and model. Retina. 2011 Sep; 31(8):1609–19. [PubMed: 21844839]
4. Marmor MF, Hu J. Effect of disease stage on progression of hydroxychloroquine retinopathy. JAMA Ophthalmol. 2014 Sep; 132(9):1105–12. [PubMed: 24922444]
5. Itoh Y, Kaiser PK, Singh RP, et al. Assessment of retinal alterations after intravitreal ocriplasmin with spectral-domain optical coherence tomography. Ophthalmology. 2014 Dec; 121(12):2506–2507. [PubMed: 25208855]
6. Oishi A, Hata M, Shimozono M, Mandai M, Nishida A, Kurimoto Y. The significance of external limiting membrane status for visual acuity in age-related macular degeneration. Am J Ophthalmol. 2010 Jul; 150(1):27–32. [PubMed: 20609705]
7. Coscas, et al. IOVS 2015 Restoration of Outer Retinal Layers After Aflibercept Therapy in Exudative AMD: Prognostic Value.
8. Rodriguez-Padilla JA, Hedges TR 3rd, Monson B, Srinivasan V, Wojtkowski M, Reichel E, Duker JS, Schuman JS, Fujimoto JG. High-speed ultra-high-resolution optical coherence tomography findings in hydroxychloroquine retinopathy. Arch Ophthalmol. 2007 Jun; 125(6):775–80. [PubMed: 17562988]
9. Mititelu M, Wong BJ, Brenner M, Bryar PJ, Jampol LM, Fawzi AA. Progression of hydroxychloroquine toxic effects after drug therapy cessation: new evidence from multimodal imaging. JAMA Ophthalmol. 2013 Sep; 131(9):1187–97. [PubMed: 23887202]
10. Singh RP, Li A, Bedi R, Srivastava S, Sears JE, Ehlers JP, Schachat AP, Kaiser PK. Anatomical and visual outcomes following ocriplasmin treatment for symptomatic vitreomacular traction syndrome. Br J Ophthalmol. 2014 Mar; 98(3):356–60. [PubMed: 24357495]
11. Ehlers JP, Itoh Y, Xu LT, et al. Factors associated with persistent subfoveal fluid and complete macular hole closure in the PIONEER study. Invest Ophthalmol Vis Sci. 2014 Dec 18; 56(2): 1141–6. [PubMed: 25525173]

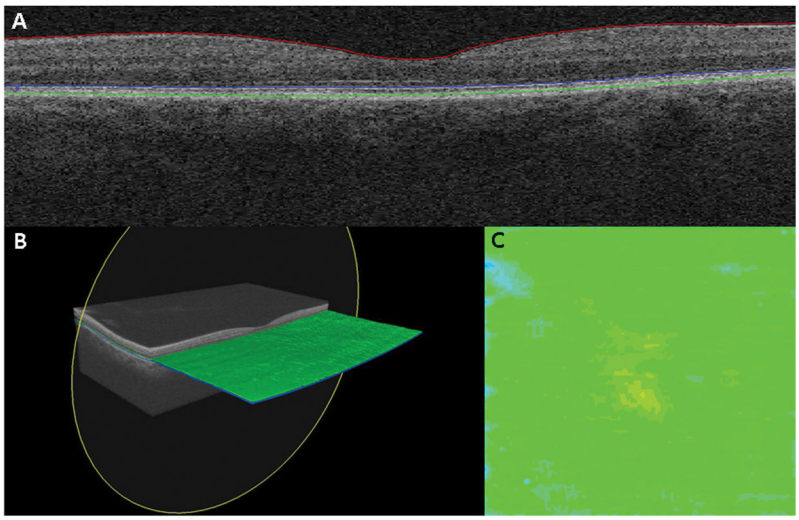

Figure 1.

Ellipsoid zone mapping in a normal eye. (A) B-scan segmentation of the ellipsoid zone. (B) Three-dimensional reconstruction of the ellipsoid zone revealing the overall integrity (green). (C) *En face* mapping of relative ellipsoid zone to retinal pigment epithelium thickness.

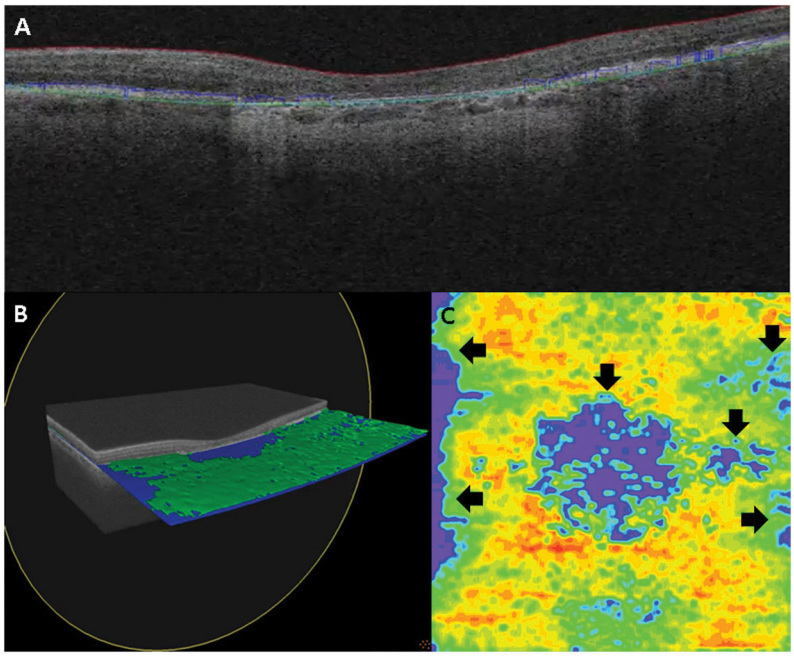

Figure 2.

Ellipsoid zone mapping in an eye with geographic atrophy secondary to age-related macular degeneration. (A) B-scan segmentation of the ellipsoid zone. (B) Three-dimensional reconstruction of the ellipsoid zone revealing the overall integrity (green) and areas of ellipsoid zone loss (blue). (C) *En face* mapping of relative ellipsoid zone to retinal pigment epithelium thickness, note the reduced ellipsoid zone to retinal pigment epithelium thickness (arrows)

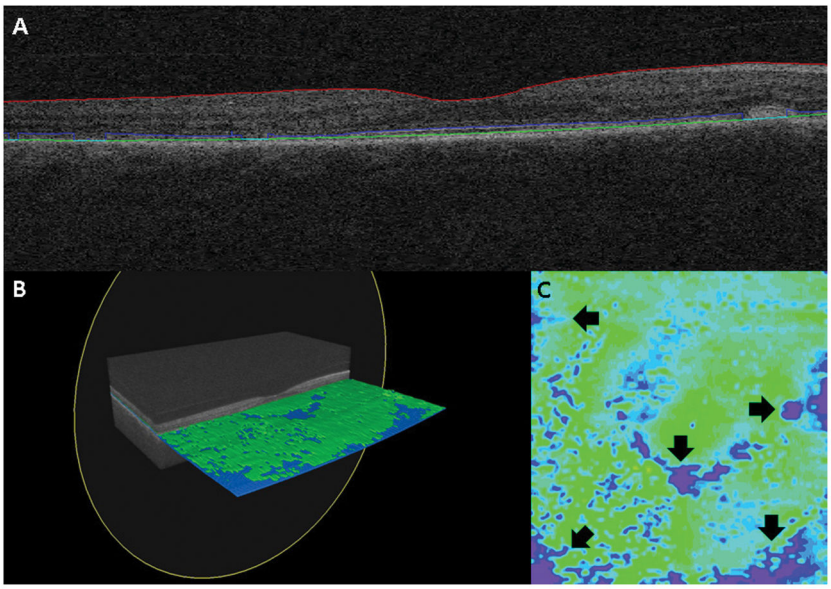

Figure 3.

Ellipsoid zone mapping in an eye with early hydroxychloroquine toxicity. (A) B-scan segmentation of the ellipsoid zone. (B) Three-dimensional reconstruction of the ellipsoid zone revealing the overall integrity (green) and areas of annular ellipsoid zone loss (blue). (C) *En face* mapping of relative ellipsoid zone to retinal pigment epithelium thickness, note the reduced ellipsoid zone to retinal pigment epithelium thickness (arrows)

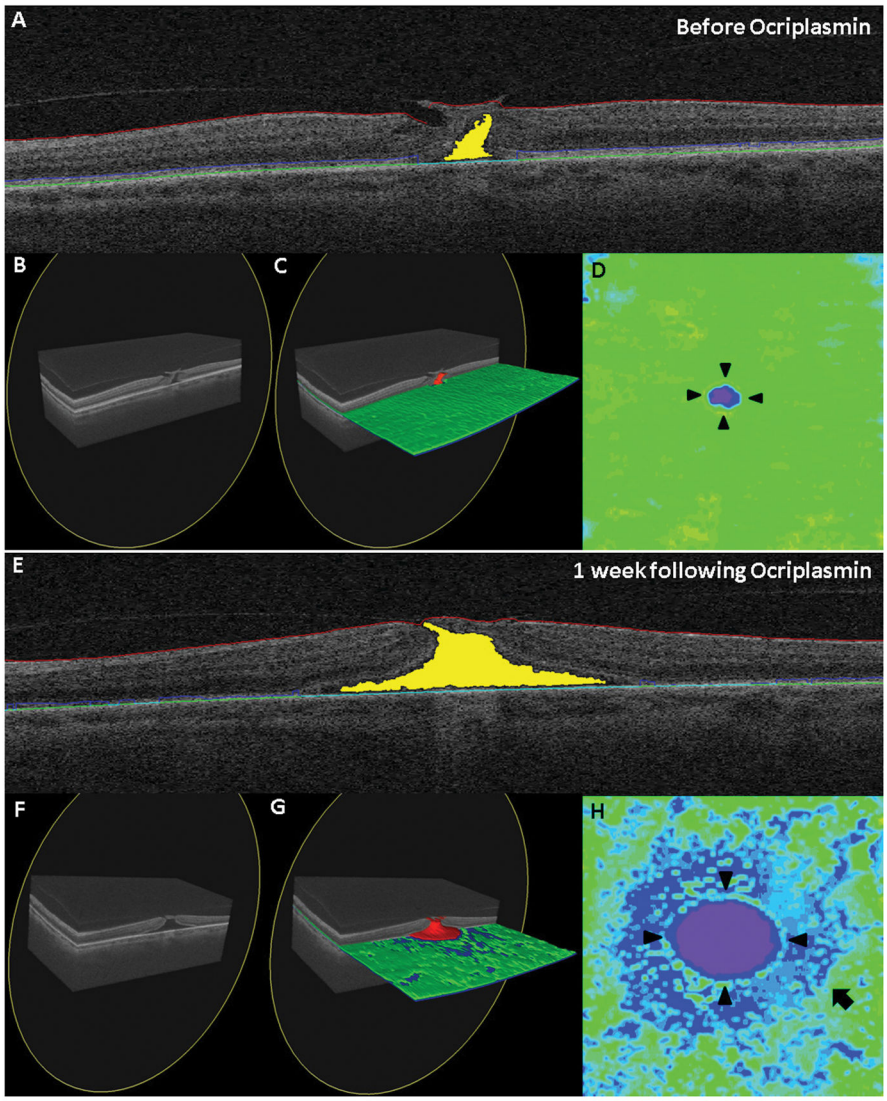

Figure 4.

Ellipsoid zone mapping in an eye prior to and after ocriplasmin injection. (A) B-scan segmentation of the ellipsoid zone prior to ocriplasmin injection. (B, C) Three-dimensional reconstruction of the ellipsoid zone revealing the overall ellipsoid zone integrity (green) and automated segmentation/reconstruction of macular hole (red). (D) *En face* mapping of relative ellipsoid zone to retinal pigment epithelium thickness, note the absent ellipsoid zone in area of macular hole. (E) B-scan segmentation of the ellipsoid zone following ocriplasmin injection. Note significant increase in subretinal and macular hole size (yellow). (F, G) Three-dimensional reconstruction of the ellipsoid zone revealing the overall ellipsoid zone integrity (green) and multi-focal areas of ellipsoid zone loss (blue). Macular hole enlargement is also identified (red). (H) *En face* mapping of relative ellipsoid zone to retinal pigment epithelium thickness, note the expansion ellipsoid zone loss in area of enlarged macular hole and the diffuse heterogenous thinning of the ellipsoid zone.

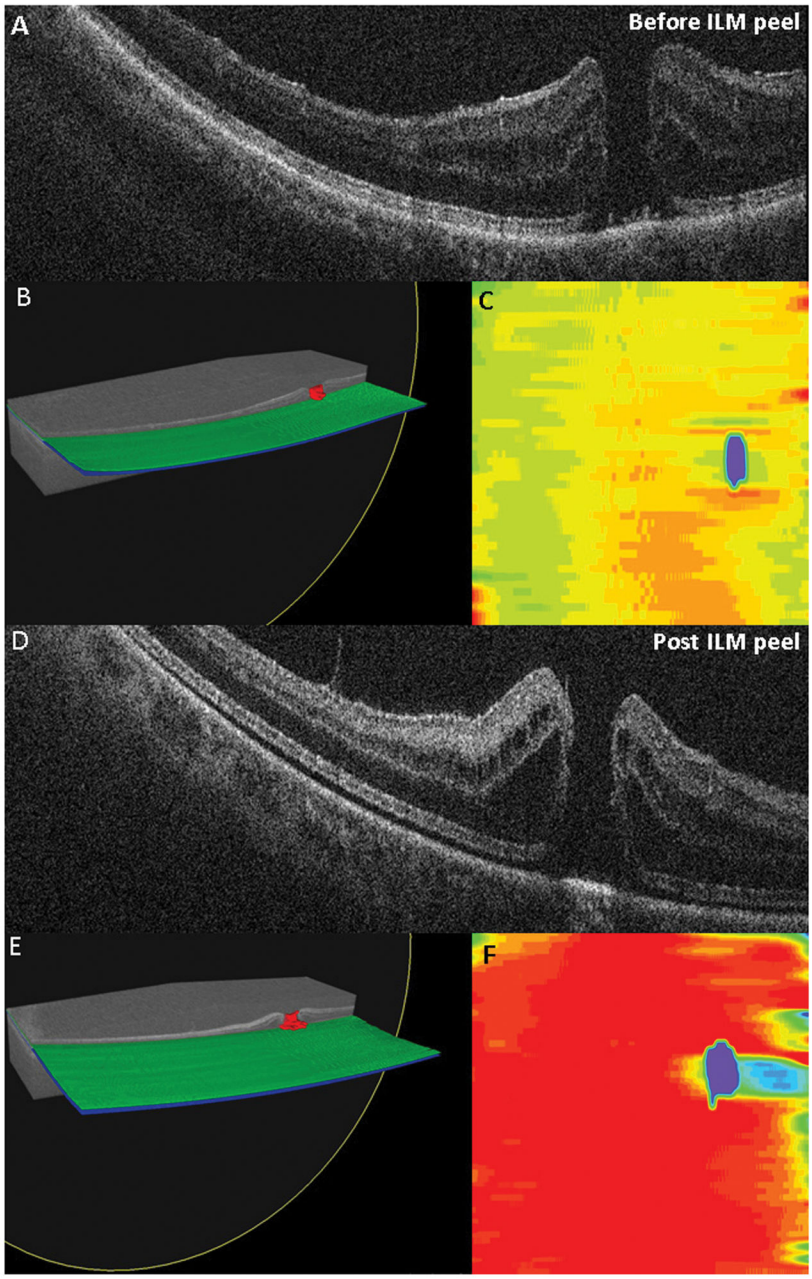

Figure 5.

Ellipsoid zone mapping with intraoperative optical coherence tomography scans before and after internal limiting membrane (ILM) peeling in a macular hole case. (A) B-scan prior to ILM peeling showing typical ellipsoid zone to retinal pigment epithelium height. (B) Three-dimensional reconstruction of the ellipsoid zone revealing the overall integrity (green) and segmented macular hole (red). (C) *En face* mapping of relative ellipsoid zone to retinal pigment epithelium thickness. (D) Following ILM peeling, B-scan reveals expansion of the ellipsoid zone to retinal pigment epithelium height. (E) Three-dimensional reconstruction of the ellipsoid zone revealing the overall maintained integrity (green) and segmented macular

hole (red). (F) *En face* mapping of relative ellipsoid zone to retinal pigment epithelium thickness, note marked diffuse increased ellipsoid zone to retinal pigment epithelium height.